Molecular dynamics simulations of the indentation of a crystalline surface by an atomic force microscope tip

R. Ferrando, M. Andrei, A. Relini, R. Rolandi, and A. Gliozzi
Dipartimento di Fisica, Universita' di Genova, Via Dodecaneso 33, 16146 Genova, Italy
(Received 2 March 2005; published 7 July 2005)

The indentation of protein crystals by an atomic force microscope tip is studied by molecular-dynamics simulations. This work is inspired by our previously reported experimental results, showing the occurrence of force jumps in the contact region of force-distance curves measured on ferritin crystals. These jumps were interpreted as due to the removal of molecules from the surface. Here we perform simulations of the indentation of topmost crystal layers with different tip sizes; special attention is devoted to the case corresponding to the experimental conditions, in which the tip size is twice the size of the crystal molecules. Force-distance curves are calculated. These curves show a first clear jump in correspondence of the rupture of the first layer; this jump is associated to the removal of a few molecules from the surface. The jump height, the curve shape, and the emission mechanism of the molecules from the crystal depend strongly on the indentation point. In particular, the amplitude of tip jumps resulting from crystal layer breakage is found to have a multimodal distribution. These results are in agreement with the interpretation previously given to our experimental results.

DOI: 10.1103/PhysRevB.72.045412 PACS number(s): 68.35.Fx, 68.35.Gy

I. INTRODUCTION

Nanotechnology and nanoscience development requires understanding material properties at the nanometer scale. When the relevant length scales of an experiment are in the submicron range, anisotropic effects due to the molecular order become important and single molecule interaction must be considered rather than collective interaction.

Material mechanical properties, and in particular plastic deformation, are often studied by indentation tests. To study indentation at nanometer scale (nanoindentation), the atomic force microscope (AFM) is used. This instrument, originally designed for high resolution imaging, is capable to measure forces in the nano-Newton scale and its probe, which is a sharp tip connected to a cantilever, can be used as a nanometer size indenter.[1–8] In a typical AFM indentation experiment, the tip is approached to the sample, makes contact with it, indents it, and eventually is retracted to its original position. The force acting on the probe is recorded as a function of the probe displacement, yielding a force-distance curve.

We used this technique to study the nanomechanical properties of protein crystals, with the aim of obtaining information about intermolecular forces. These are of paramount importance in the crystallization process, which is often made difficult by the want of physical information. Protein crystals are important in modern biosciences since their availability has traditionally encouraged the development of structural studies aimed to the elucidation of links between protein structure and function.

We focused our attention on ferritin crystals.[9,10] Ferritin is a 470 kD protein responsible for iron storage. It is formed by 24 identical subunits, each of 174 residues, assembled into a nearly spherical shell, providing a cavity where up to 4500 Fe atoms can be stored as insoluble Fe(III) hydroxide. The shell, which is the repeating unit in the crystal, has a radius close to 7 nm and therefore comparable to the tip radius. Ferritin crystallizes in a cubic lattice, which reflects the high symmetry of the protein oligomer. Crystals display an octahedral habit; therefore, all faces are equivalent, corresponding to (111) crystal planes.

Performing indentation experiments on this system we faced a few limitations of the technique. The information that can be extracted during the AFM indentation process is limited to the force between the tip and the sample and often it is not possible to observe indentation effects. In principle, after indentation, the damaged surface can be observed in the imaging mode. However, information about the molecular displacements and rearrangements are not easily accessible. For these reasons, computer simulation is a very valuable tool to investigate the microscopic aspects of the indentation process.

The oldest indentation simulations were performed several years ago.[11,12] Nowadays, nanoindentation simulations are mostly used for studying nucleation and dislocations dynamics inside a crystal indented by a rigid tip.[13–16] Such simulations are mostly intended to study the effect of a deep indentation of the sample, involving the breaking of many crystal layers, focusing on the formation of dislocations inside the crystal. These studies were related to the indentation of metallic samples. Komvopoulos and Yan[17] simulated the indentation of a few layers of a metallic substrate calculating the force-distance curves for some representative cases. However, a systematic study of the indentation initial stages and their dependence on the indentation site is still lacking. This is due to the fact that, in the case of metallic crystals, the typical curvature radii of the indenters, usually larger than 10 nm, are much greater than the size of metal atoms, which are on the order of 0.2 nm. Therefore, it can be understood that positioning the AFM tip above different points of the surface unit cell of the crystal cannot cause different indentation behaviors.

Having in mind the indentation experiments on ferritin crystals,[9] we used molecular dynamics simulations to model

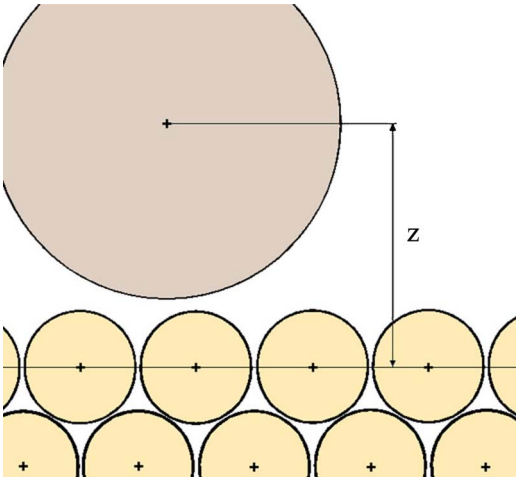

FIG. 1. (Color online) Schematic representation of the tip-crystal system, with indication of the tip vertical displacement z. The tip is represented by the large sphere.

the indentation of a crystal surface by an AFM tip, whose curvature radius has a size comparable with the repeating unit of the crystal. The dependence of force-distance curves on the indentation point and the underlying atomistic mechanisms of rearrangement are investigated.

II. MODEL AND METHODS

Due to the complex structure and high molecular weight of ferritin, a simulation of a ferritin crystal taking explicitly into account each individual atom of each ferritin molecule is at present impossible. Therefore, a coarse-grained modeling is necessary. In ferritin crystals the repeating unit is the

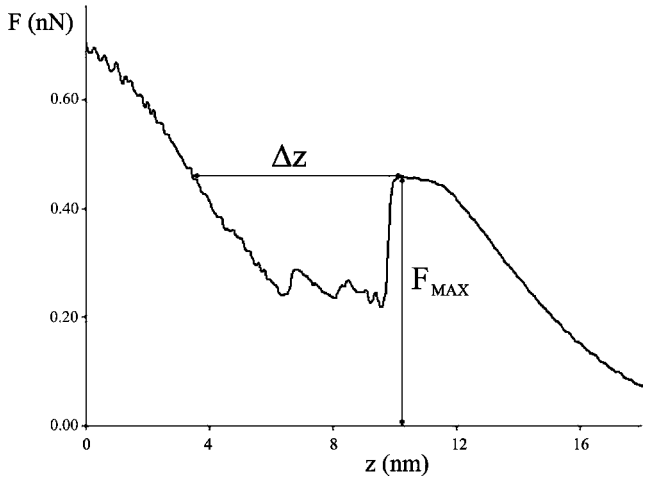

FIG. 2. Simulated force-distance curve. The force (F) acting on the tip is plotted as a function of the tip vertical displacement (z). F_{MAX} is the maximum value the force reaches before the first layer breakage, which corresponds to the force abrupt decrease. Δz is the tip advancement necessary to reach again F_{MAX}. It corresponds to the amplitude of tip jump during the layer breakage. Simulation conditions: bridge indentation position, $t/m=2$, approach speed 10 cm/s.

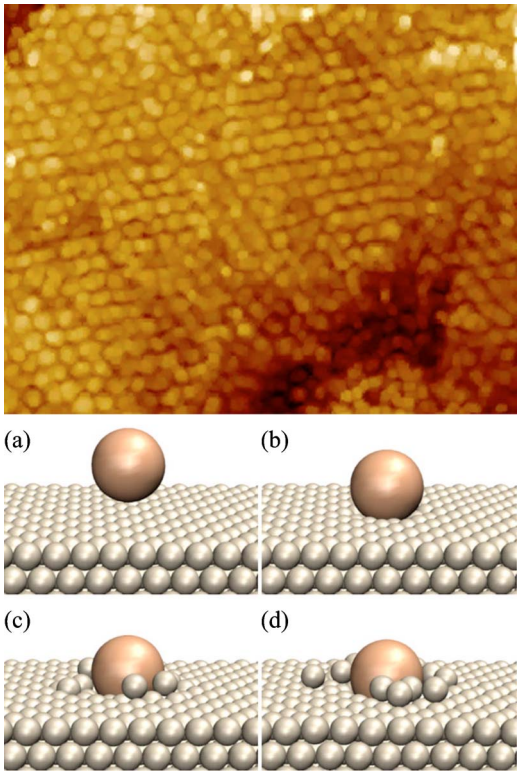

FIG. 3. (Color online) A spherical tip approaches the crystal surface: (a) the tip is far from the surface; (b) the tip, pushing on the surface, induces an elastic deformation of the crystal surface; (c) the first layer starts breaking, the crystal lattice is deformed and three molecules are removed from the crystal surface; (d) the tip has reached the second layer and several molecules are removed from the surface. A tapping mode AFM image of a ferritin crystal surface at molecular resolution (height data) is also shown. Scan size, 400 nm$\times$320 nm; Z range 3 nm. The experimental conditions are described in Ref. 9.

spherical shell, which is an oligomer. Since here we will treat the ferritin oligomer as a single molecule, in the text we will refer to it as the "molecule." When dealing with globular proteins, it is usually assumed[18–20] that molecules are spherically symmetric particles whose mutual interaction is approximated by a Lennard–Jones 6–12 potential V:

$$V(r) = \varepsilon\left[\left(\frac{r^*}{r}\right)^{12} - 2\left(\frac{r^*}{r}\right)^{6}\right],$$

where r is the distance between the considered particles, ε is the depth of the potential energy minimum, and r^* the intermolecular distance to which it corresponds. The value $\varepsilon = 7.6\times10^{-2}$ eV has been provided from growth experiments of ferritin crystals performed by Yau *et al.*[20] The equilibrium distance between the molecules, in agreement with x-ray diffraction data[10] is assumed to be 13.3 nm; moreover, thermal expansion has been taken into account.[21]

Experimental observations[9] evidenced the ferritin crystals being arranged in a fcc structure with exposed faces corresponding to (111) crystal planes (see the AFM image in Fig. 1). Therefore, our simulation slab will expose a (111) surface in the x-y plane, where periodic boundary conditions have

been applied. Many test simulations have been performed to establish the appropriate number of particles to be included in the slab. We have found that a reasonable size to permit reproducibility of the results is about one thousand particles. The particles in the lowest layer have been kept fixed.

A spherical tip geometry was considered, since we were interested in indenting only a few layers. Indentations realized with different tip shapes (cylindrical, conic, pyramidal) gave results that are analogous to the spherical case, provided that the radius of curvature in the contact zone is equal.

The tip-molecule potential has been chosen to be solely repulsive. This is due to two reasons. First, we are interested in the indentation of the crystal, and this involves essentially the repulsive part of the tip-sample interaction. Second, in the experimental force-distance curves for ferritin indentation, no jump-to-contact was recorded.[9] This indicates that the attractive part of the interaction is weak. Concerning the repulsive part, we have performed a number of tests by changing the exponent of the power-law repulsion from 12 to 96. These tests have shown a qualitative independence of the results from this exponent.

Two types of simulations have been carried out. The first type is a Molecular Dynamics simulation at constant temperature. The equations of motion have been integrated making use of the Velocity–Verlet algorithm,[22–24] with a time step much smaller than the molecular vibrational period. The temperature has been kept constant by an Andersen thermostat.[25]

The simulations of the second type have been conducted making use of a quenching technique. Such a method consists in considering the advancement of the tip toward the crystal, splitting it up into a definite number of discrete steps. At each step, the tip is kept fixed, and the coordinates of the atoms in the slab are relaxed to the closest local potential energy minimum. This procedure permits us to understand in detail the behavior of the particle system apart from the thermal motion.

Our results have shown a substantial correspondence among the results of the two types of simulations. Quenching simulations have been especially useful to reveal the rearrangement pathways in the crystal, as we shall see in the following.

III. RESULTS AND DISCUSSION

A. Constant velocity approach

In this section we describe the results obtained bringing the tip near the sample with a constant speed. Such an approximation is equivalent to assume an infinitely rigid cantilever and an infinite mass of the tip-cantilever system. Although these approximations may seem unrealistic, they lead to results consistent with a more realistic model (vide infra), with the advantage of saving computing time, especially in quenching simulations. Force-distance curves have been plotted calculating the resulting force exerted on the tip by the crystal, in correspondence of each value of the tip-sample distance. The simulated force-distance curves show jumps (abrupt force decreases) similar to those found in the experimental curves obtained on ferritin crystals.[9] Figure 2 shows the typical behavior of a simulated force-distance curve. F_{MAX} is the maximum value which the force reaches before the jump; Δz is the distance required for the tip advancement to reach the value of F_{MAX} again.

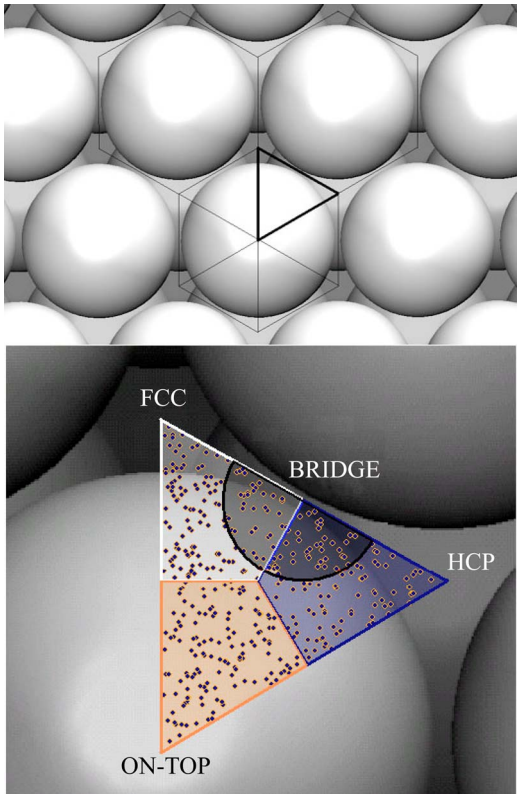

FIG. 4. (Color online) Upper panel: fcc(111) surface, with a triangle representative of the lattice unit cell. Lower panel: the triangle in a larger view field. The triangle is divided in the four regions considered to classify the indentation positions. The crystal sites, which the regions are named from, are also indicated.

On the basis of our experimental results,[9] we expected a tip size effect. Therefore, we performed simulations with different tip sizes. We indicate the ratio between tip and crystal molecule radii as t/m ratio. Our simulations employ t/m ratios ranging from 1 to 10. In the case of t/m ratios <5, simulation movies show that jumps correspond to particle removal from the surface (Fig. 3); in particular, the first jump corresponds to the rupture of the first crystal layer. Jumps occur when the particles that are directly in contact with the tip move to allow tip advancement. These particles may either leave the crystal surface or exchange their positions with neighbor particles, which, in turn, leave the surface.

To investigate the dependence of F_{MAX} and Δz on the indentation site, we simulated experiments in which the indentation sites were randomly chosen inside a triangular domain representative of the unit cell of the (111) surface. We have distinguished different indentation regions, named from on top, fcc, hcp, and bridge sites, as represented in Fig. 4. The bridge region partially overlaps fcc and hcp regions.

In Figs. 5(a) and 5(b) the indentation positions are represented with different grey levels corresponding to the values of Δz resulting from the simulated force-distance curves. In

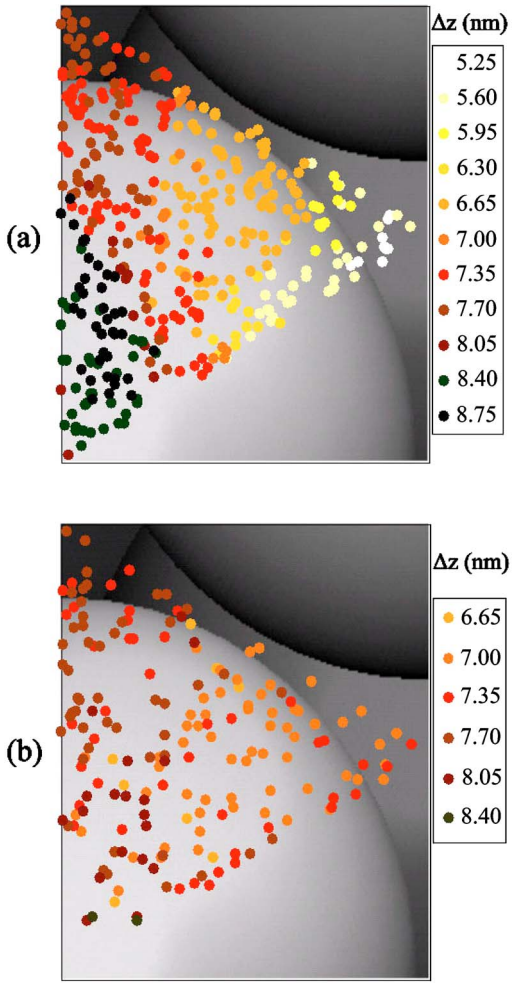

FIG. 5. (Color online) Δz as a function of indentation position. Δz values are reported in the grey (color) scale indicated in the insets. (a): 400 indentations with $t/m=2$; (b): 200 indentations with $t/m=5$. The tip approach velocity is of 10 cm/s.

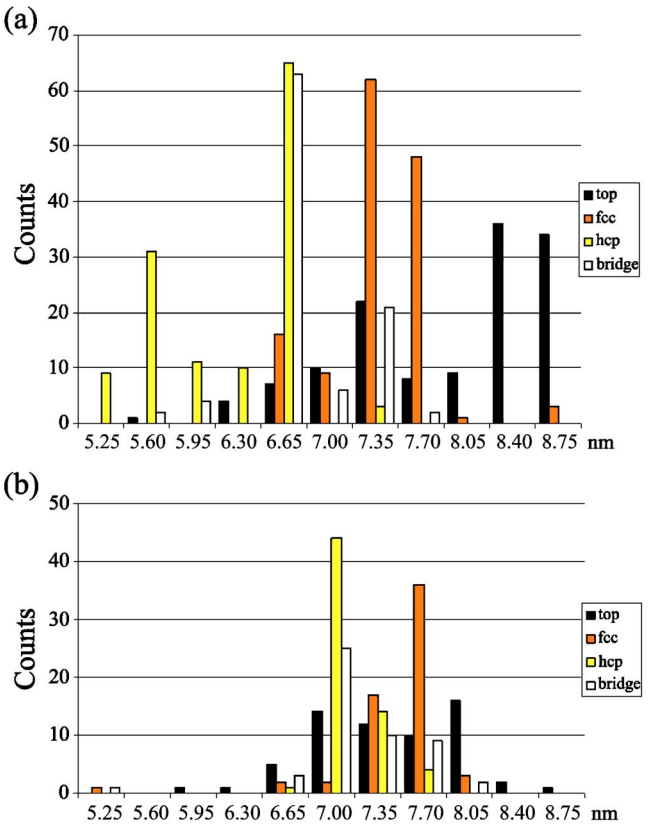

FIG. 6. (Color online) Histograms of Δz, corresponding to the indentations of Fig. 5. Different grey (color) levels correspond to different indentation regions (see inset). Panel (a) 400 indentations, $t/m=2$; panel (b) 200 indentations, $t/m=5$.

Fig. 5(a), corresponding to a t/m ratio of 2, similar Δz values are obtained in the neighborhood of each surface site; Δz values are in the range between 5.25 and 8.75 nm. For a t/m ratio equal to 5 [Fig. 5(b)], the Δz range is narrower (from 6.65 to 8.40 nm) and the correlation between the Δz values and the indentation regions is less evident. The histograms of Δz values obtained for t/m ratios equal to 2 and 5 are reported, respectively, in Figs. 6(a) and 6(b). Contributions arising from different indentation regions are represented with different grey levels. A lower t/m ratio corresponds to a more evident multimodality of the distribution of Δz.

The main reason for different Δz values corresponding to different tip advancement is the different number of molecules removed from the surface. This is evident studying the detailed movements of the particles involved during indentation. Figure 7 shows typical sequences of snapshots of the indentation process on the most representative surface sites in the case of t/m ratio equal to 2. In all the cases, the emitted particles are not those which are in direct contact with the tip. In fact, particle emission takes place by exchange processes analogous to those found in surface diffusion.[26] When the tip is positioned on the bridge site [Fig. 7(a)], its advancement displaces two molecules, labeled A and B in the figure; molecules A and B replace C and D, which are pushed off the surface. In the case of the fcc indentation [Fig. 7(b)], a larger number of molecules is involved. The molecules A, B, C, located at the vertices of the triangle representative of the unit cell, rotate counterclockwise displacing the molecules D, E, and F which are pushed off the crystal surface. The hcp indentation is similar, but the molecules at the triangle vertices do not rotate and simply replace the neighbor molecules D, E, F [Fig. 7(c)]. From Figs. 5(a) and 6(a) the measured Δz turns out to be greater for fcc indentation than hcp indentation, even though in both cases the number of removed particles is 3. This is explained by the fact that although fcc and hcp sites do not differ at the level of the topmost layer, they differ for the arrangement of molecules in the second layer and this gives rise to different indentation processes. In the on top indentation [Fig. 7(d)], the molecule below the tip is pushed in the second layer. With a domino effect, molecule B from the second layer replaces molecule C in the first layer; molecule C replaces molecule D, which leaves the crystal surface. In this case there is a further emission of particles, which is not shown in Fig. 7(d) and is described in Fig. 8.

Figure 8 shows the force and the number of removed particles as a function of tip advancement for fcc and on-top indentations in the case of a t/m ratio equal to 2. In the case

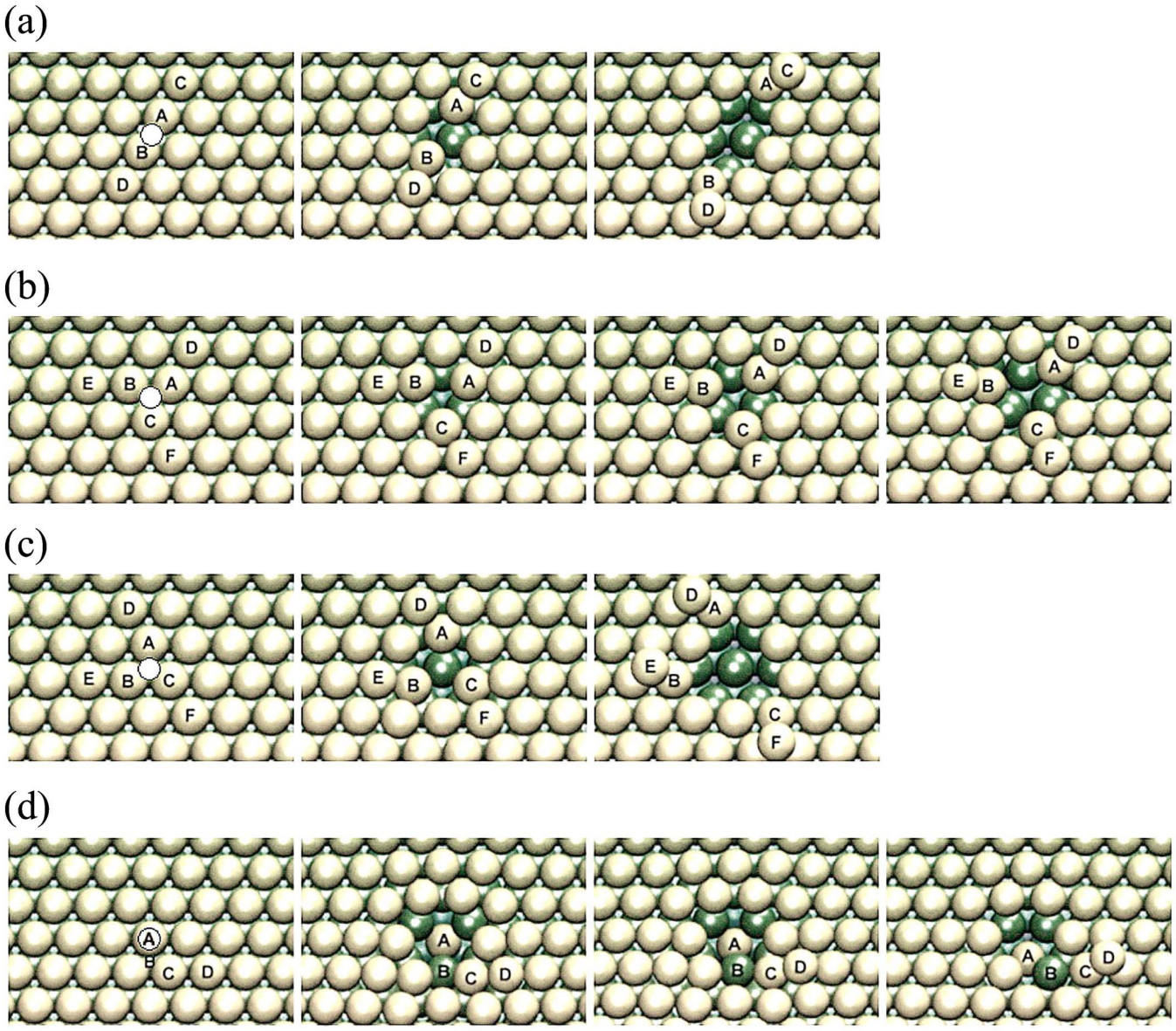

FIG. 7. (Color online) Snapshots of the indentation processes in different crystal sites from quenching simulations, for $t/m=2$. The white spot indicates the indentation position. Second layer molecules are represented as being darker. Panel (a), bridge position: the tip pushes molecules A and B that force out C and D from the crystal surface. Panel (b), fcc position: molecules A, B, and C are first forced to rotate counterclockwise and force out D, E, and F. Panel (c), hcp position: molecules A, B, and C, without rotating, force out D, E, and F. Panel (d), on-top position: initially, the tip pushes A inside the crystal, distorting the crystal lattice. Then, with a domino effect, molecule B from the second layer replaces molecule C in the first layer; molecule C replaces molecule D, which leaves the crystal surface. In this case there is a further emission of particles, which is not shown here and is described in Fig. 8.

of fcc indentation (light grey), three molecules are removed immediately after the maximum of the force is reached. In the case of on top indentation, the first force decrease does not correspond to the emission of molecules but to a deformation of the crystal lattice. The molecule below the tip is pushed inside the second crystal layer. This rearrangement is similar to that observed more often for larger tips, for which it may take place irrespective of indentation position, that is not only for on-top indentation. Subsequently, in correspondence of the larger force decrease, up to ten molecules are removed from the surface. Finally, a few molecules relocate so that the net amount of removed molecules is 7. In Fig. 9 different grey levels correspond to different values of F_{MAX}; also in this case a correlation between F_{MAX} and the indentation position is observed. A larger tip radius results in larger values of F_{MAX}. The F_{MAX} percentage variation, with respect to the mean value, passes from 10% in case (a) to 4% in case (b), and the tendency is to vanish for greater tip sizes, as seen for Δz. Interestingly, the highest value of F_{MAX} is obtained indenting in the fcc site for a t/m ratio equal to 2 and in the hcp site for a t/m ratio equal to 5.

The simulation results are in agreement with the interpretation given previously[9] to our experimental results. The experimental force-distance curves, obtained indenting a fer-

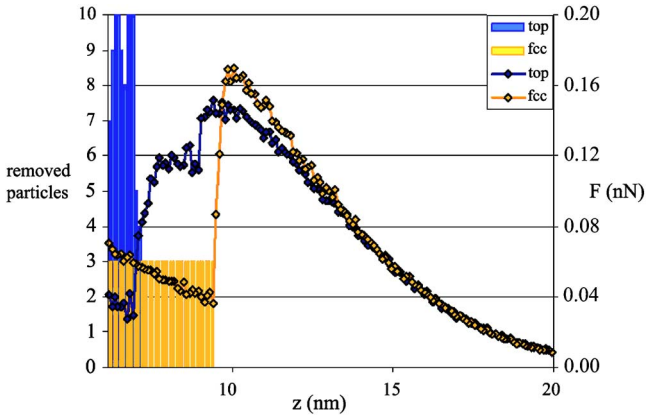

FIG. 8. (Color online) Force-distance curves and corresponding number of removed particles for fcc (light grey (orange)) and on-top indentations (black). In fcc indentation three particles are immediately forced out of the crystal. In on-top indentation a molecular rearrangement takes place (small jump), followed by the removal of several molecules. A few molecules go back to the surface and the final number of removed molecules is seven. Conditions: $t/m=2$, approach velocity 10 cm/s.

ritin crystal with an AFM tip whose curvature radius was about twice the molecule radius showed the occurrence of force jumps in the contact region. These jumps were interpreted as due to the removal of molecules from the surface. The statistical distribution of the corresponding Δz had a multimodal character,[9] suggesting a place dependency of the removal mechanism. This hypothesis was not verified experimentally since it was not possible to obtain a direct evidence of molecular removal by imaging the crystal at molecular resolution before and after indentation. This might be due either to the difficulty of a precise tip repositioning after an approach/withdrawal cycle and/or to the possibility that subsequent to molecule displacement, surface molecular arrangements take place.

The multimodal distribution of Δz obtained from the simulations is qualitatively in agreement with that measured in the experiments; however, smaller values of Δz were obtained in the experiments.[9] Therefore, we have performed simulations adding a further, much smaller sphere on top of the original tip, in order to model the presence of impurities or defects of the tip in the contact zone. We have obtained multimodality of Δz even for large t/m ratios: the radius of the added sphere determines the behavior of the system during indentation. However, the values of Δz are larger than the experimental ones also in this case.

To study the effect of temperature, we performed simulations with temperatures ranging from 0 to 300 K (results not shown). Temperature does not affect the general behavior of the system in an appreciable way; as expected, as temperature increases, F_{MAX} values decrease.

B. Tip-cantilever system treated as a harmonic oscillator

The AFM probe is not a rigid system, since the tip is connected to a cantilever which is bent by the force exerted on the tip by the sample. Therefore, in an approach/withdrawal cycle, the tip velocity is not constant. In the previous model, we neglected the cantilever action. To check the results of our simulations, we introduced a spring constant to simulate the presence of the cantilever. This model is more realistic but it requires more computing time, because the convergence of the quenching simulations is more difficult. While an end of the spring proceeds at a constant velocity, the motion of the tip (connected to the other end of the spring) is determined by the action of the sample and by the spring restoring force. A finite mass was associated to the spring-tip system and located in correspondence of the tip. Experimentally, the tip-cantilever resonance frequency rather than the mass is known. In our AFM experiments, the resonance frequency in aqueous environment was typically about 6 kHz. We estimated the effective mass, that takes into account the displaced mass of the fluid,[27] from the resonance frequency by using a spring constant value of 0.06 N/m.[9] The probe oscillation period is enormously longer than the vibrational periods in the sample. Moreover, it is not possible

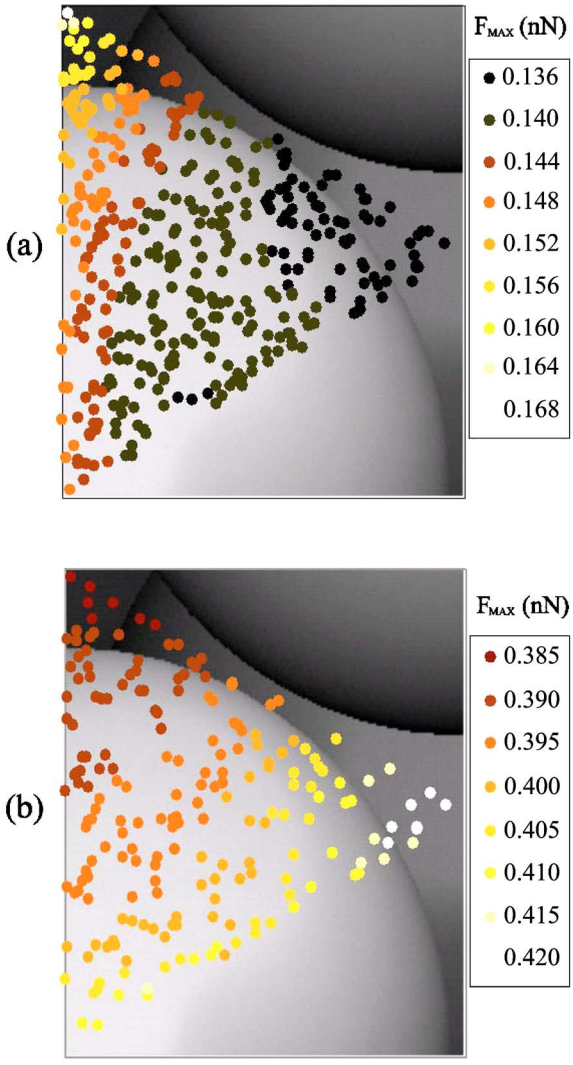

FIG. 9. (Color online) F_{MAX} as a function of indentation position for the same simulations of Fig. 5. F_{MAX} values are reported in the grey (color) scale indicated in the insets. (a): 400 indentation with $t/m=2$; (b): 200 indentations with $t/m=5$.

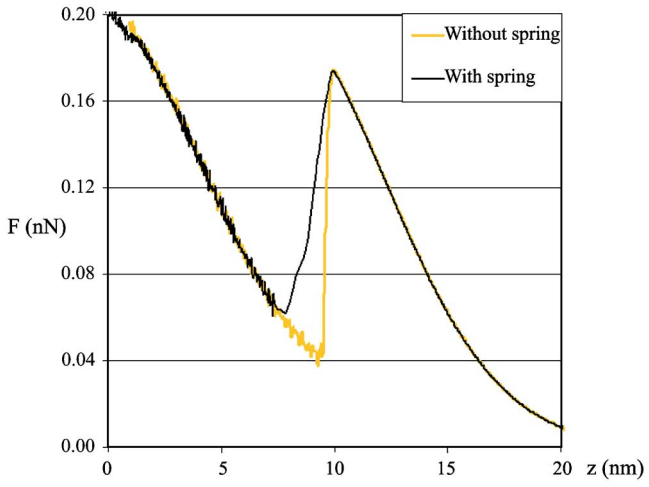

FIG. 10. (Color online) Comparison of force-distance curves obtained for two different models: light grey (yellow), constant velocity approach; black, tip-cantilever system treated as a harmonic oscillator. $t/m=2$; fcc indentation, tip approach velocity 10 cm/s.

to simulate an approach at experimental velocity. For these reasons, we had to modify these two parameters. The criterion employed was to keep the ratio between resonance frequency f and approach speed v equal, in the experimental and simulated case

$$\frac{f_{\text{sim}}}{v_{\text{sim}}} = \frac{f_{\text{exp}}}{v_{\text{exp}}}.$$

Since the experimental approach speed was $v_{\text{exp}}=2640$ nm/s, we considered a resonance frequency of $f_{\text{sim}}=225$ MHz, and an approach speed $v_{\text{sim}}=10$ cm/s. These values were chosen after tests performed with lower velocities and corresponding lower resonance frequencies, which provided the same qualitative results.

To prevent the system oscillation, we used a quality factor Q on the order of unity. Simulations with greater Q values did not provide different results. The damping has been realized applying to the tip-cantilever mass an Andersen thermostat[25] which gives, with such a high damping, the same results as applying Brownian dynamics.[28]

Figure 10 compares the force-distance curves produced by the harmonic oscillator and by the constant speed models. It is evident that the parameters F_{MAX} and Δz are not affected by the method chosen to simulate the system.

C. Indentation of hard-core molecules

In order to investigate the dependence of the force-distance curves on the interaction between crystal molecules, we have introduced a hard core region in the Lennard–Jones interaction potential

$$V(r) = \varepsilon\left[\left(\frac{r^* - r_{\text{min}}}{r - r_{\text{min}}}\right)^{12} - 2\left(\frac{r^* - r_{\text{min}}}{r - r_{\text{min}}}\right)^{6}\right].$$

r_{min} is the radius of the hard core region, that is the minimum approach distance between two particles; the standard Lennard–Jones formulation is obtained for $r_{\text{min}}=0$. The potential energy minimum is given by $V(r^*)=-\varepsilon$. Although the energy minimum is the same as in the Lennard–Jones potential and is located at the same distance, the wall of the potential well is steeper. Force-distance curves, obtained for bridge indentations with $t/m=3$ and for different values of r_{min}, are shown in Fig. 11. The three jumps correspond to the breakage of subsequent layers. Larger hard cores result in higher values of F_{MAX} and increased kinetic energy of the outgoing particles, owing to the higher potential energy stored before breakage. As expected, the values of Δz also depend on the hard-core radius.

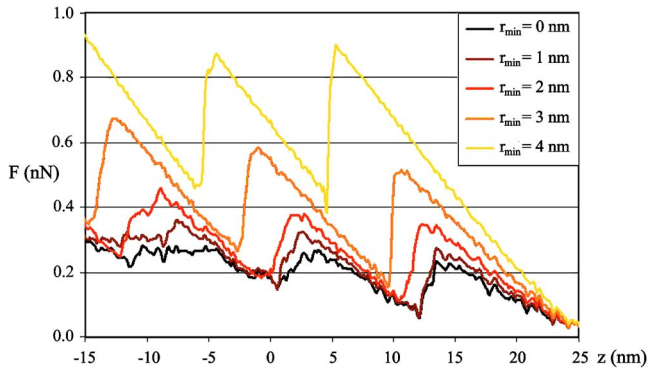

FIG. 11. (Color online) Force distance curves obtained with the hard core model. Different grey (color) levels correspond to different values of r_{min}. The three jumps correspond to the indentation of three different crystal layers. All curves refer to bridge indentation, $t/m=3$, and tip approach velocity 20 cm/s.

IV. CONCLUSIONS

Our simulations describe the indentation mechanism of a protein crystal by an AFM tip, when the tip and crystal molecules sizes are in the same order of magnitude. The results indicate that a jump in the force-distance curve is produced in correspondence of the first crystal layer breakage. The final result of the breakage is the removal of a few molecules, usually from the first layer. In some cases [Figs. 5(a), 5(b), and 8] the molecule removal is immediate and corresponds to a single jump in the force-distance curve. In other cases [Fig. 5(b)] the indentation process comprises two steps. In the first step the crystal lattice is distorted or rearranged; in the second a few molecules leave the surface. These steps correspond to multiple jumps in the force distance curve (Fig. 8). This behavior is more often found with large tips (results not shown). For small tips, a correlation is observed between the indentation site and (a) the values of Δz; (b) the values of F_{MAX}; (c) the number of molecules removed. This finding supports the interpretation given to the experimental results reported in Ref. 9.

In AFM experiments, the dependence of the force-distance curves on the indentation site opens the possibility to identify the indentation site with respect to the crystal surface, provided that the probe radius is comparable with molecule size. From the experimental point of view, site identification could not be straightforward, since the presence of small defects on the tip may affect the effective value of the tip radius.

ACKNOWLEDGMENTS

The authors acknowledge financial support from the Italian MIUR under the Project PRIN 2003028141_005. Molecular dynamics have been obtained with VMD, a molecular graphics program originally designed for the interactive visualization and analyses of biological materials, developed by the Theoretical Biophysics Group in the Beckman Institute for Advanced Science and Technology at the University of Illinois at Urbana-Champaign (Ref. 29).

[1] G. Binnig, C. F. Quate, and C. Gerber, Phys. Rev. Lett. **56**, 930 (1986).
[2] Y. Choi, K. J. Van Vliet, Ju Li, and S. Suresh, J. Appl. Phys. **94**, 6050 (2003).
[3] S. Haque, Surf. Eng. **19**, 255 (2003).
[4] M. R. Van Landingham, J. S. Villarrubia, W. F. Guthrie, and G. F. Meyers, Macromol. Symp. **167**, 15 (2001).
[5] B. Bushan and X. D. Li, Int. Mater. Rev. **48**, 125 (2003).
[6] B. Cappella and G. Dietler, Surf. Sci. Rep. **34**, 1 (1999).
[7] W. R. Bowen, R. W. Lovitt, and C. J. Wright, Biotechnol. Lett. **22**, 893 (2000).
[8] N. Agraït, G. Rubio, and S. Vieira, Phys. Rev. Lett. **74**, 3995 (1995).
[9] V. Mollica, A. Relini, R. Rolandi, M. Bolognesi, and A. Gliozzi, Eur. Phys. J. E **3**, 315 (2000).
[10] V. Mollica, A. Borassi, A. Relini, O. Cavalleri, M. Bolognesi, R. Rolandi, and A. Gliozzi, Eur. Biophys. J. **30**, 313 (2001).
[11] U. Landman, W. D. Luedtke, N. A. Burnham, and R. J. Colton, Science **248**, 454 (1990).
[12] U. Landman and W. D. Luedtke, J. Vac. Sci. Technol. B **9**, 414 (1991).
[13] K. Michielsen, M. T. Figge, H. De Raedt, J. Th. M. De Hosson, and E. van der Giessen, in *Advances in Computational and Experimental Engineering and Sciences, Proceedings of ICES03, 2003*, edited by C. A. Herrera (Tech. Science Press, Forsyth, GA, 2003).
[14] K. J. van Vliet, J. Li, T. Zhu, S. Yip, and S. Suresh, Phys. Rev. B **67**, 104105 (2003).
[15] D. Feichtinger, P. M. Derlet, and H. van Swygenhoven, Phys. Rev. B **67**, 024113 (2003).
[16] X.-L. Ma and W. Yang, Nanotechnology **14**, 1208 (2003).
[17] K. Komvopoulos and W. Yan, J. Appl. Phys. **82**, 4823 (1997).
[18] P. R. Wolde and D. Frenkel, Science **277**, 1975 (1997).
[19] R. P. Sear, J. Chem. Phys. **111**, 4800 (1999).
[20] S. T. Yau, D. N. Petsev, B. R. Thomas, and P. G. Vekilov, J. Mol. Biol. **303**, 667 (2000).
[21] S. H. Choi and S. Maruyama, *Calculation of Heat Conduction of Solid by Classical Molecular Dynamics Methods*, 39th National Heat Transfer Symposium of Japan, Sapporo 2002.
[22] M. P. Allen and D. J. Tildesley, *Computer Simulation of Liquids* (Claredon, Oxford, 1987).
[23] W. F. van Gunsteren and H. J. C. Berendsen, Mol. Phys. **45**, 637 (1982).
[24] D. Frenkel and B. Smit, *Understanding Molecular Simulations* (Academic Press, New York, 1997).
[25] H. C. Andersen, J. Chem. Phys. **72**, 2384 (1980).
[26] T. Ala-Nissila, R. Ferrando, and S. C. Ying, Adv. Phys. **51**, 949 (2002).
[27] G. Chen, R. Warmack, T. Thundat, D. P. Allison, and A. Huang, Rev. Sci. Instrum. **65**, 2532 (1994).
[28] R. Ferrando, F. Montalenti, R. Spadacini, and G. E. Tommei, Chem. Phys. Lett. **315**, 153 (1999).
[29] W. Humphrey, A. Dalke, and K. Schulten, *VMD—Visual Molecular Dynamics*. J. Mol. Graphics **14**, 33 (1996).